ABSTRACT

Title of Document	Velocity based Defrost of Evaporator Coils of Heat pumps
	Kamalakkannan Muthusubramanian Master of Science, 2015
Directed By	Professor. Michael M. Ohadi Department of Mechanical Engineering

Defrosting of the outdoor coils of residential heat pumps in an energy efficient manner remains an active area of research in the HVAC industry. Inverting the cycle to reject heat from the outdoor coils is the most common method used currently. However, this method is energy intensive. The current study proposes a novel method that can substantially reduce the energy consumed in such defrost cycles. It involves controlled use of reverse air flow on the outdoor coil surface during the defrost cycle, providing better cleaning of the coil surface by improving draining of the melted frost and removal of frost without the need to melt it, resulting in fewer defrost cycles needed for a given duration of heat pump operation. Energy savings of 56% and 31% were demonstrated experimentally for the above- and below-freezing environments respectively, as compared to a baseline that represents the ASHRAE recommended operating conditions.

VELOCITY BASED DEFROST OF EVAPORATOR COILS OF HEAT PUMPS

By

Kamalakkannan Muthusubramanian

Thesis submitted to the Faculty of the Graduate School of the
University of Maryland, College park, in partial fulfillment
of the requirements for the degree of
Master of Science
2015

Advisory Committee:
Dr. Michael M. Ohadi, Chair (Professor, Department of Mechanical Engineering)
Dr. Marino diMarzo
Dr. Amir Riaz

ACKNOWLEDGEMENTS

My most sincere thanks go to my advisor, Dr. Michael M. Ohadi for all of his support. Dr. Ohadi gave me the opportunity to join the S2TS lab two years ago as a graduate student, and conduct this research. His guidance and encouragements have supported and helped me throughout my graduate education.

I would like to thank Dr. Serguei V. Dessiatoun and Dr. Amir H. Shooshtari. Dr. Serguei & Dr. Amir advised and guided me throughout this research and supported me with the day to day efforts in making progress. Their insight on how to set up experiments and trouble shoot problems during the research has taught me much.

My thanks go to my committee members, Dr. diMarzo and Dr. Riaz. I appreciate both of them for being in the committee.

Thanks to all of my colleagues at the S2TS lab, I thank all of you for your help, support and friendship.

Finally, I would like to thank my family and friends who have supported me during this entire two year period.

TABLE OF CONTENTS

LIST OF FIGURES

LIST OF TABLES

NOMENCLATURE

Symbol	Description	Units
$C_{p,\ F}$	Specific heat of working fluid	(kJ/kg K)
E	Electrical energy used by the fan	(kJ)
I	Current drawn by the fan	(A)
$\dot{m}_F$	Mass flow rate of working fluid	(kg/s)
ΔP	Differential pressure	(Pa)
$Q_{defrost}$	Thermal energy supplied during defrost	(kJ)
$T_{F,in}$	Working fluid temperature in to heat exchanger	(°C)
$T_{F,out}$	Working fluid temperature out of heat exchanger	(°C)
Δt	Time steps	(s)
ΔT	Measured differential temperature	(°C)
V	Velocity	(m/s)
V_{DC}	DC voltage supplied to the fan	(V)
ω	Humidity ratio of air	(-)

1. INTRODUCTION

The two heat exchanger coils of a common vapor compression cycle operate at two temperature levels. During normal winter operation, the outdoor coil operates as an evaporator. The refrigerant in this coil receives heat from the low temperature outdoor ambient air, which is forced to flow over it using a fan. During this heat exchange process, the air temperature typically drops below the dew point and the water vapor in the air condenses. The condensed droplets separate out of the air and reside on the surface of the evaporator coil leading to formation of frost. Frost is detrimental to the performance of the heat pump. It increases the resistance to heat transfer by adding a layer of low thermal conductivity ice on the surface of the evaporator coil. It also increases the pressure drop across the coil. Moreover, the temperature lift, defined as the difference between the two temperature levels of the heat pump, shrinks as frost grows on the outdoor coil. As a result, the performance of the heat pump cycle measured in terms of the coefficient of performance (COP) drops.

Figure 1: An example photograph of frost formation on the outdoor coil of heat pump. (Source of picture: www.takaiser.com)

Researchers have explored various options such as dehumidifying using desiccant materials and surface coating to reduce frost formation, these options are discussed in section 2.

Frost formation cannot be eliminated altogether. A major part of the heat of evaporation comes from the condensing water vapor. Since the latent heat of water is much larger than the sensible heat, it is possible to run a vapor compression cycle with a reasonable volume of moist air flowing across the evaporator coil. If dry air were to be used, the volume of air needed for the same amount of heat of evaporation would be a lot larger, and this would imply that larger physical equipment for the same capacity would be required. Therefore, the requirement of the phase change process on the surface of evaporator can lead to formation of frost.

Defrosting and draining of the frost from time to time is necessary to maintain the performance of the heat pump. There are many known methods to defrost the evaporator coil, such as off cycle defrosting, electric defrosting, hot gas defrosting and reverse cycle defrosting. A prominent method in industry is reverse cycle defrosting. In this method, the direction of refrigerant flow and the direction heat flows in the heat pump are inverted. The evaporator coil now works as the condenser coil and heat is rejected. This rejected heat provides the energy needed to defrost the accumulated frost on the surface of the coil.

The reverse cycle defrost method is incorporated into the operation sequence of the heat pump using various control strategies. Two popular strategies are “time-based defrosts” and “control-based defrosts” [1, 2]. The time-based defrost initiates and terminates a defrost cycle periodically at fixed time intervals, whereas the control-based defrost initiates and terminates defrost cycles based on set points assigned to some measurable process parameter. The general aim of the reverse cycle defrost method with either of the control strategies is to melt all the frost and depend on gravity to remove liquid droplets from the surface of the evaporator coil.

The current industrial practice is to turn off the outdoor fan during defrost cycle. This is in line with the recommendations of ASHRAE [1]. Thus there is no forced air flow on the outdoor coil during the defrost cycle. However, it has been noted that low gravitation force and surface interaction of water droplets and coil surface generally result in accumulating residual water on the coil, extending the defrosting cycle and increasing defrosting energy.

This research involves study of a novel method to run defrost cycles with the use of air flow on the outdoor coil surface. The experiments simulated the frost formation and defrost cycles. The experiments were based on the reverse cycle defrost method. Both time-based defrost strategy and control-based strategy were simulated. All experiments were run in environmental conditions that have been recognized as the worst frosting conditions with temperatures in the range of -5º C to +5º C and over 70% RH [1]. The experiments were classified as above-freezing and below-freezing experiments to evaluate the proposed method in this worst frosting condition. It was found experimentally that when using the proposed methods that use airflow on the coil surfaces during defrost cycle, the energy needed for the defrost process decreased and the residual water on the coil surface decreased, providing better cleaning as compared to the experiments that were run with the defrost method recommended by ASHRAE.

2. LITERATURE REVIEW

Muthusubramanian et al. [3] investigated the effect of using air flow during the heating and defrosting cycles of a heat pump. It was reported that increasing the velocity of air flow during the simulated heating cycle retarded the rate at which frost grows on the evaporator coil. During the simulated defrost cycle, it was reported that using air flow in the direction opposite to the normal direction of air flow on the evaporator coil provides an energy saving opportunity. It was concluded that such use of reverse air flow increased the time interval between subsequent defrosting. A reduction of about 50% in the number of defrost cycles needed in a given time period of heat pump operation was reported.

The effect of surface coating using hydrophilic and hydrophobic materials was investigated by Jhee et al [4]. They reported that with the use of hydrophilic surface coating, the amount of frost accumulation increased by 4.9% and with hydrophobic surface coating, frost accumulation increased marginally by 0.4%. They noted that heat exchangers with hydrophobic surface treatment were more effective in terms of defrosting efficiency and time. The amount of residual water on the hydrophobic surface treated heat exchanger was shown to be smaller than that of the bare heat exchanger. They reported that the water draining rate during defrost was enhanced by 3.7% and 11% with hydrophilic and hydrophobic surface treatments, respectively. The fact that more frost accumulates during frosting dilutes the benefits during defrosting for hydrophilic surface coats.

Vocale et al. [5] conducted a numerical analysis to investigate the influence of the outdoor air temperature and relative humidity on the energy performance of heat pumps. The number of defrost cycles needed was analyzed with real world data acquired from various sites where the temperature was in the range of -5 ºC to +5 ºC and relative humidity (RH) was between 50% to 90%. They noted that relative humidity had a higher influence on frost formation as compared to temperature. They reported that the COP of heat pumps decreased by 17% in wet outdoor conditions with RH > 80% and temperatures in the range of 0 ºC to 6 ºC.

Wang & Liu [6] proposed the use of solid adsorbent bed as a method to prevent frost formation. This method reduced the relative humidity and increased the temperature of the air, which in turn led to reduced frost formation. They noted that as the bed adsorbed moisture, its performance dropped and the air RH would increase gradually. Special construction was required to install the adsorbent bed and for continuous operation, regeneration of the bed was also necessary.

An innovative method to reduce frost formation by using electric field was reported by Tudor et al. [7]. The principle was to generate localized non-resistive heating within fins of an evaporator coil by the application of a high-voltage, alternating current through electrodes. It was reported that the defrosting time was substantially reduced when this method was adopted. This method required installation of electrodes in-between the heat exchanger fins, which could be a complex fabrication activity. The voltages and frequencies at which this method would be optimum were not reported.

J.M. Hang et al. [8] conducted a numerical study of the effects of frost thickness on heat transfer of finned tube heat exchanger and recommended that defrost should occur when half of a single flow channel area is blocked by frost. It was also concluded that use of centrifugal fan and axial fan had similar results on the heat transfer rates for a large fin pitch heat exchanger under frosting condition. S. Roy et al. [9] studied the defrosting on an inclined surface using hot air jet impinges and developed a correlation for defrosting as a function of time and impinging angle. They also proposed a joule heating defroster and numerically simulated it. The result of their simulation showed substantial reduction in defrosting time to the extent of 70%. Using this method for a residential heat pump evaporator coil for defrosting would need special construction. Y. Yao et al [10] developed a mathematical model to study the performance of the airside heat exchanger under frosting in an air source heat pump. The result of this study showed that at a constant temperature the defrosting interval increases with increase in relative humidity. They also reported that at constant relative humidity the frost formation is more serious at a high temperature than at low temperature when the heat pump is operating under certain temperature levels.

3. PROJECT OBJECTIVES

The current industrial practice is to turn off the outdoor fan during the defrost cycle. It was thought that the cold outdoor air may prolong the defrost process and if the ambient is below freezing point, defrost will not be completed at all.

The objective of this research was to use air flow in the direction opposite to the normal direction of the air flow during the defrost cycle to explore energy savings opportunity in the defrost cycle. These opportunities were studied at the worst frosting conditions.

Exploring the possibility of dislodging layers of frost without melting it using the reverse air flow was the first objective of this research. Figure 2 shows this possibility.

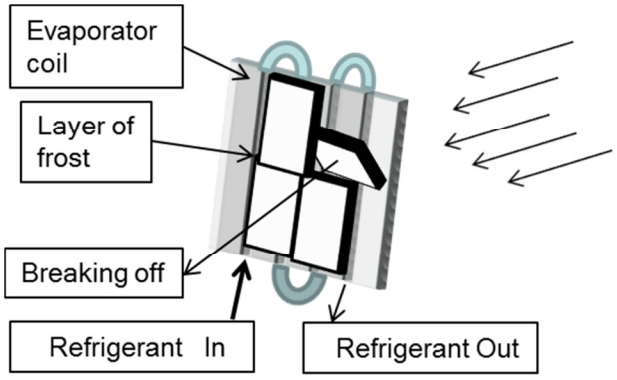

Figure 2: Layers of frost breaks off from the evaporator coil before the expenditure of thermal energy to melt it due to the flow of reverse air

In the above freezing environment the moving stream of air could reduce the time interval of a defrost cycle by increasing the rate at which the accumulated frost melts.

Exploring this possibility was the second objective of the project. Figure 3 shows this possibility.

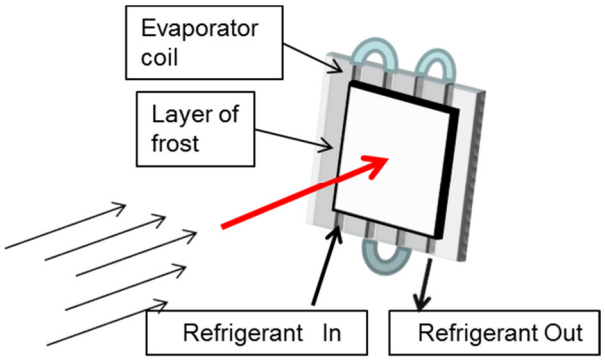

Figure 3: Moving stream of air contributing to the melting process in the above freezing environment, the red arrow indicates heat transfer from ambient air to the frost

The amount of residual water droplets on the coil surface after the defrost cycle can be reduced if the moving stream of air improves the draining of the coil. Reduction in the amount of residual water droplet would impact the time interval between subsequent defrost cycle. Exploring the possibility to increase the time interval between subsequent defrost cycles using the reverse air flow was the third objective of the research.

As mentioned in section 1 and 2, researchers have explored the possibility of reducing the frost formation on the coil surface. Exploring the possibility to make changes to air velocity during the frost formation cycle to reduce or retard frost formation was the fourth objective of the research.

4. EXPERIMENTAL SET UP

In order to simulate the frost formation cycles and defrost cycles, an experimental test rig was set up. A heat exchanger was used to replicate the evaporator coil on which frost was allowed to grow in a controlled environment. Defrost was controlled by adopting the two control strategies introduced in section 1. Various instruments were used to measure test parameters. The list of instruments used is summarized in Table 1. The schematic of the test set up is shown in Figure 4.

Table 1: Instruments used in the experimental set up

Instrument	Range	Accuracy
Differential Pressure	0 to 5 inch water column	± 0.14%
Anemometer	0 to 8 m/s	± 5%
T type Thermocouple	-270 to 400ºC	± 0.5ºC
Humidity sensor	0 to 100 %	± 5%
Float type flow meter	0 to 100% (100% = 0.78 GPM of water)	± 2%

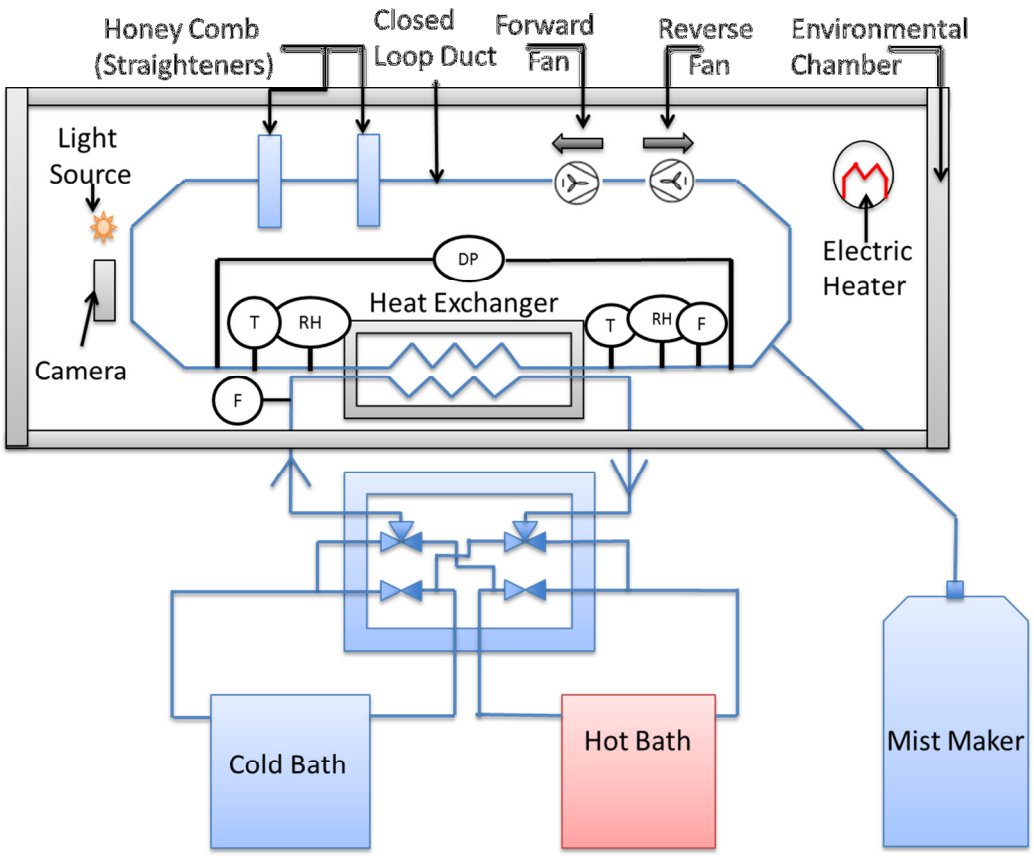

Figure 4: Schematic of Experimental Set Up

The experiment was set up in an environmental chamber. The temperature and relative humidity inside the environmental chamber were maintained by an electric heater and a mist maker respectively. A closed loop duct was housed inside the environmental chamber. In the top half of the loop, two fans were installed, a forward and a reverse fan. The fans were installed so that the directions of air flow were opposite to each other. Two honeycomb straighteners were used in the air flow path on the discharge side of the forward fan. The purpose of the straighteners was to ensure that the air was distributed uniformly on the upstream side of the heat exchanger so that the frost formation would be

uniform. The heat exchanger that represents the evaporator is housed in the bottom half of the closed loop duct.

Generally, the evaporator of the vapor compression cycle has a refrigerant which undergoes phase change in the normal and defrost cycles. To replicate the heat transfer process in this study, two refrigerated baths in conjunction with an equal mixture of water and ethyl alcohol in single-phase mode were used. These baths maintained the working fluid at two different temperatures. This was needed to simulate the frost formation condition and defrost cycles. The cold bath pumped the working fluid at temperatures that replicated the normal heating cycles of the heat pump. The warm bath pumped the working fluid at temperatures that replicated the defrost process.

The set-up had a valve arrangement. The valve arrangement had two purposes. First, it created a recirculation flow path for the working fluid when it was not being pumped to the heat exchanger coil. Second, it facilitated the online switching over from simulated heating mode to the simulated defrost mode or vice versa. The working fluid was pumped out of the respective baths; it flowed through the valve assembly and was either recirculated back to the bath or was passed through a float type flow meter to eventually flow into the test section. From the test section, it circulated back into the bath.

A differential thermocouple was built and calibrated to accuracy of 0.06 ℃. The differential temperature as defined in Eq. (1) was measured directly using this differential thermocouple.

$$\Delta T = T_{F,out} - T_{F,in} \tag{1}$$

This differential thermocouple had four junctions in each stream. Using such differential thermocouple increases the accuracy of measurement by reducing the errors due to noise and cold end compensation [11-14].

Other important components in the setup included two DC power supplies for the fans, an electric heater, a data logger for the measurements, a camera, and lighting inside the environment chamber to record the events as they happened.

The various components used in the experiment are shown in Figure 5 through Figure 24.

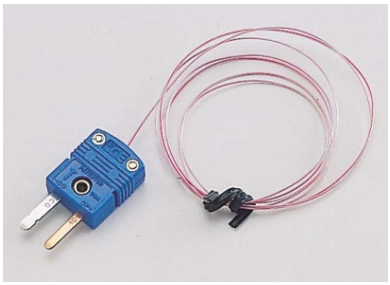

Figure 5: T type thermocouple

Figure 6: Temperature controller

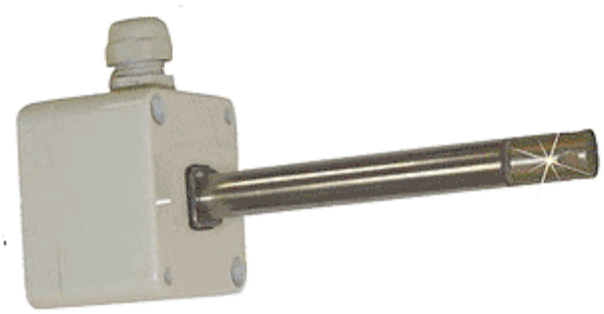

Figure 7: Humidity Sensor

Figure 8: Humidity Controller

Figure 9: Differential Pressure Sensor

Figure 10: Anemometer

Figure 11: Forward fan

Figure 12: Reverse fan

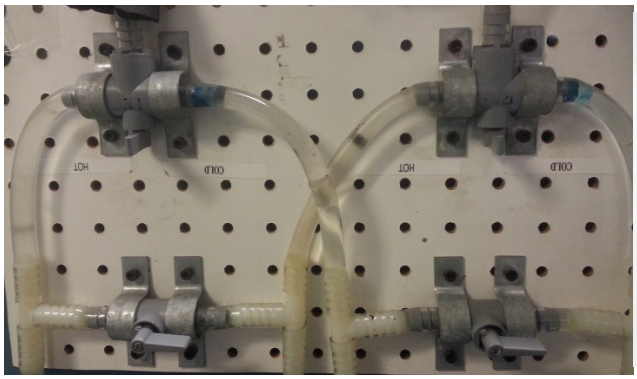

Figure 13: Valve Arrangement

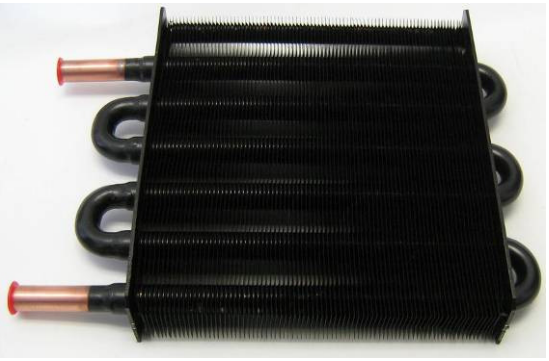

Figure 14: Heat Exchanger Coil

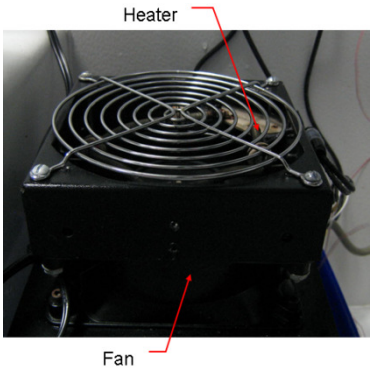

Figure 15: Electric Heater and fan

Figure 16: Mist Maker

Figure 17: Power supply for reverse fan

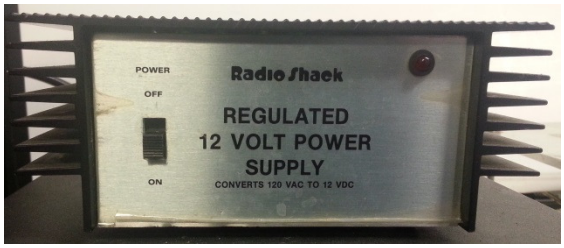

Figure 18: Power supply for forward fan

Figure 19: Warm bath

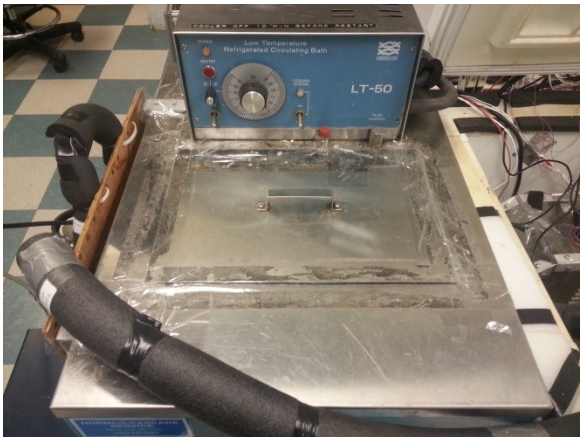

Figure 20: Cold bath

Figure 21: Float type flow meter

Figure 22: Webcam

Figure 23: Data logger

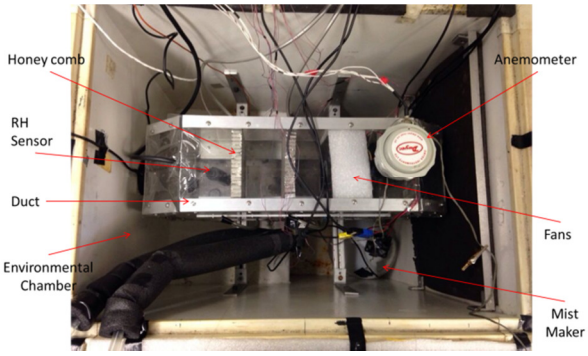

Figure 24: Environmental Chamber

5. EXPERIMENTS

5.1 Experimental Test Procedure

At the start of each experiment, it was necessary to bring the set up to the required test conditions. When the experiment conditions were achieved in the environmental chamber and the working fluid baths, the experiment began and simultaneously the data logger and the video recorder were started to collect data for analysis.

At the start of the experiment, the working fluid from the cold bath was pumped through the valve arrangement and float type flow meter to the heat exchanger where heat transfer would take place. The working fluid would circulate back to the bath from the heat exchanger. The forward fan moved air across the heat exchanger in the closed loop duct. This was the simulated heating cycle of the heat pump. Since the experiments were done in single phase mode, the working fluid temperature increase could be monitored and the heat transferred to the working fluid estimated. As frost grew on the surface of the heat exchanger, the flowing air experienced higher resistance; this caused an increase in differential pressure across the heat exchanger. Simultaneously, there was a decrease in the differential temperature between the incoming and the outgoing stream of the working fluid because of the increase in thermal resistance to heat transfer introduced by the layer of frost.

The termination of the simulated heating cycle and initiation of the defrost cycle was based on the control strategy adopted for the particular experiment. To start the defrost process, the valves were switched so that the working fluid from the hot bath was pumped to the heat exchanger while the working fluid from the cold bath was kept in

recirculation mode. Frost melted during the defrost process. Termination of the defrost cycle also depended on the control strategy chosen for the particular experiment.

5.2 Time based defrost cycle

The time-based defrost cycle is the most reliable but least energy efficient defrost strategy [2]. A defrost cycle is initiated after a specific duration of heat pump operation in the heating mode. Typical time intervals are 30, 60 or 90 minutes depending on the heat pump manufacturer and the geographic location of the installation. The defrost cycle lasts for a specific duration, typically 10 minutes [1, 2]. The outdoor fan is turned off during this defrost cycle.

The above strategy was adapted to our experiment such that frost was allowed to grow on the surface of the coil for 90 minutes during the simulated heating cycle. The defrost cycle was initiated at the end of this 90-minute period. The duration of the defrost cycle was selected as 1 minute. This interval was selected after running the defrost cycles a few times and visually observing the defrosting process and identifying the duration needed in the experimental setup.

The outdoor fan is usually turned off during defrost cycle because it is thought that the cold outdoor air may prolong the defrost process, and if the ambient is below freezing point, defrost will not be completed at all. However, in our adoption of the time-based defrost strategy, the reverse air fan was used continuously during the defrost cycle. That is, the reverse air fan was used during the entire 1 minute of the defrost cycle. The idea was to explore the opportunity to dislodge a part of the frost from the coil surface without supplying heat energy to melt it fully. Another reason for using the reverse air fan during

the defrost cycle was to explore the opportunity to remove the residual water droplets that reside on the coil surface at the end of conventional defrost cycles, which otherwise can be only partially drained with gravitational force.

The experimental test conditions for these experiments are summarized in Table 2. The results of the experiments run with this control strategy are discussed in section 6.1.

Table 2: Test conditions for time based defrost control strategy experiment run at above freezing environment conditions

Air Temperature	2º C
Relative Humidity	90 %
Working fluid Temperature(Cold Bath)	-8º C
Working fluid Temperature (Hot Bath)	20º C
Duration of Frost Growth	90 minutes
Reverse Air Velocity	5 m/s

Air flow in the forward direction during the defrost cycle was not considered, as it did not prove to be beneficial (see section 6.5).

5.3 Modified time based defrost strategy

Based on the results discussed in section 6.1, the time-based control strategy discussed in section 5.2 was modified for further experimentation. In the modified time-based control strategy the duration of the defrost cycle was reduced to 40 seconds. Further, since the focus of this study was on the defrost cycle and energy used in the defrost cycle, the frost formation phase of the experiment was modified such that the simulated heating cycle was terminated when the differential pressure across the evaporator coil exceeded a set point. This is similar to the frost formation phase of the control based defrost strategy discussed in section 5.4.

The 40-second defrost cycle would complete defrost when reverse air fan was used during the defrost cycle. This is demonstrated in the result discussed in section 6.1. . The idea was to show that 40 seconds would be insufficient when the fan is turned off during defrost cycle.

Two experiments were set up to compare the energy requirements during the defrost cycles run with the conventional defrost method and the proposed reverse air fan defrost method. The conventional method refers to current industrial practice in which the fan is turned off during the defrost cycle; the reverse air fan defrost is the proposed improvement in which the reverse air fan is used throughout the 40 seconds of the time-based defrost cycle. The experimental test conditions for these experiments are summarized in Table 3. The results of experimental run with this control strategy are discussed in section 6.2.

Table 3: Test conditions for the modified time based defrost strategy for both conventional and reverse air fan defrost experiment

Air Temperature	2º C
Relative Humidity	90%
Working fluid Temperature (Cold Bath)	-10º C
Working fluid Temperature (Hot Bath)	8º C
Defrost cycle duration	40 s
Reverse air flow velocity	5.5 m/s

5.4 Control based defrost cycle

Control-based strategies are the most common choice in industry these days. The control-based defrost strategy differs from the time-based defrost strategy in the sense that both the defrost cycle initiation and termination are determined by a process parameter. When

the process parameter reaches a preselected set point value, the initiation or termination of the defrost cycles occurs. The common process parameter used for the initiation of the defrost cycle is the differential pressure across the heat exchanger. When the differential pressure exceeds a certain value, the defrost cycle is initiated. Similarly, the common parameter used for the termination of the defrost cycle is the temperature of the refrigerant exiting the heat exchanger after supplying heat to melt the frost. The differential pressure set point differs based on the heat pump manufacturer. The termination criterion is typically at the refrigerant temperature of 20 ºC (68 ºF) [1, 2]. As in the case of the time based defrost strategy, here also the fan is turned off at the start of the defrost cycle. Thus there is no forced convective heat transfer during the defrost process.

As in the case of the time-based defrost strategy, here also the fan is turned off at the start of the defrost cycle.

During the normal operation of a heat pump with no frost accumulation on the evaporator coil, the typical temperature lift is in the range of 50 to 80 ºC. The lift shrinks as frost accumulates, and at the beginning of the defrost cycle the typical temperature lift is in the range of 18 to 25 ºC. During the normal heating cycle the temperature of the refrigerant constantly drops as frost accumulates on the evaporator. At the start of the defrost cycle, the refrigerant temperature could be less than 0 ºC (32 ºF).

During the defrost cycle the refrigerant rejects the heat of condensation in the reversed cycle to melt the frost. Heat rejection continues as long as frost is being melted and the water droplets that do not fall off the coil surface after melting rise to match the

temperature of the refrigerant. Once all the frost is melted further heat rejection is not easy. At this time the internal energy of the refrigerant increases. This leads to an increase in the temperature of the refrigerant. The temperature of the refrigerant will continue to increase as long as the heat pump is operating in the defrost mode. At the set point of 20 ºC (68 ºF) the defrost cycle is terminated and normal heating operation starts [15-18].

The control-based defrost strategy was adapted to the experiment as follows:

- To initiate the defrost cycle, differential pressure set point was selected as 40 Pa
- To terminate the defrost cycle, the criteria $\Delta T = 0.1$ºC, where ΔT is given in Eq. (1) .

The set point of 40 Pa was selected after running a few experiments to identify the maximum pressure drop across the heat exchanger that is in the measurable range of the set-up.

In the experiment the working fluid was supplied from a bath which maintained a constant temperature. Since there was no phase change, the temperature of the working fluid across the heat exchanger coil changed as long as heat was rejected. When all the frost was gone and the residual water droplets reached the same temperature as the working fluid, the working fluid ΔT across the heat exchanger in the absence of natural convection and radiation approaches 0 ºC. Thus the criteria $\Delta T = 0$ ºC was the point at which defrost cycle was completed.

For the experiment, the defrost cycle termination criteria was selected as $\Delta T = 0.1$ ºC instead of $\Delta T = 0$ ºC. This is because the ΔT would not go to zero, as there is some heat

loss to ambient through natural convection and radiation. In order to study this, the working fluid was allowed to circulate through the heat exchanger in clean condition before frost was formed. The fan was turned off at this time to avoid any forced convective heat transfer. Under these conditions the ΔT was in the range of 0.04 to 0.06 ºC. Further, the experimental data also showed that the value of ΔT does not fall appreciably below 0.1 ºC.

The experiments with the control based defrost strategy were categorized into above-freezing experiments and below-freezing experiments to evaluate the proposed method in the above- and below-freezing environmental conditions. The experimental test conditions are summarized in Table 4 and Table 5 for the experiments run for the above-freezing and below-freezing environments respectively.

Table 4: Test conditions for control based strategy in above freezing environment for both the conventional and reverse air fan defrost methods

Air Temperature	+2ºC
Air RH	90%
Cold Bath Temperature	-10º C
Warm Bath Temperature	+8ºC
Reverse Air Fan Velocity	5.5 m/s

Table 5: Test conditions for control based strategy in below freezing environment for both the conventional and reverse air fan defrost methods

Air Temperature	-2ºC
Air RH	90%
Cold Bath Temperature	-14º C
Warm Bath Temperature	+8º C
Reverse Air Fan Velocity	5.5 m/s

The cold bath temperature was selected to be about 10 to 12 ºC below the environmental chamber temperature; this is based on the degree of approach requirement for evaporation to occur. The warm bath temperature was selected to be about 18 to 25 ºC higher than the cold bath; this is based on the temperature lift of the heat pump at the start of defrost cycle [1, 2, 16, 17] .

Section 6.3 discusses the results of experiments run at above-freezing environment. Section 6.4 discusses the results of experiments run at below-freezing environment.

5.5 Continuous use of reverse air flow in control based strategy

The time based defrost strategy experiments discussed in section 5.2 & 5.3 had air flowing continuously on the coil surface during defrost cycle. The results of those experiments showed that such a continuous flow of reverse air provided energy savings.

It was desired to evaluate the same idea in the control based defrost experiments also. The control strategy discussed in section 5.4 uses the differential temperature as the process parameter to terminate the defrost cycle. The same however cannot be used when the reverse air flows continuously because of the forced convective heat transfer during the defrost cycle. Thus to explore the possibility of using reverse air flow continuously during defrost cycle, a different process parameter had to be selected for the defrost cycle termination criteria.

Fan current was selected as the process parameter because it is independent of the forced convective heat transfer. The idea was, the reverse air fan's current would climb up during the defrost process and reach the full flow current value when defrost is completed

and all the residual water was drained. Thus full flow current value was the defrost cycle termination set point.

The control based defrost strategy was redefined as follows.

- To initiate the defrost cycle, differential pressure set point was selected as 40 Pa
- To terminate the defrost cycle, the criteria I = 1.85 A was selected.

The full flow current value of 1.85 A was determined by running the reverse air fan under clean conditions. The experimental condition shown in Table 4 was used for this experiment. The result of the experiment run with this criterion is discussed in section 6.7. The continuous use of reverse air flow would not be beneficial if the ambient air is below freezing, thus only above freezing conditions was evaluated with this new control strategy.

5.6 Varying air velocity during frost formation

Since the defrost cycle is energy intensive, it is desired to retard frost formation such that the interval between subsequent defrost cycles would increase. In section 2, the use of adsorbent bed, surface coat and electric charge as means to retard frost formation were discussed. In this research, the velocity of the air flowing over the evaporator coil was varied to study its impact on the frost growth rate. The idea was to increase the velocity such that the heat transfer coefficient would increase and cause the fin tip to maintain temperatures closer to the ambient air temperature. Thus in an above freezing environment the fin tip could be held at above freezing temperatures and this would effectively slow down the frost growth rate. The experiment test conditions are as

mentioned in Table 2 . Frost was allowed to grow for 90 minutes. The results of these experiments are discussed in section 6.8.

6. RESULTS AND DISCUSSIONS

The data obtained from various experiments were organized in excel spread sheets and used in a program written in Engineering Equation Solver (EES). Eq. (1) through (5) was used in this EES program to generate the results. The program was also used to estimate uncertainty of calculated parameters.

Sections 6.1 through 6.8 discuss the various results of the experiments. Section 7 discusses the setting up of the error propagation function in EES.

6.1. Time based defrost strategy – Visual observation

Visual observation from the experimental setup using the method described in section 5.2, showed that it was indeed possible to use the reverse air fan during the defrost cycle and dislodge layers of frost without melting it. Figure 25 is a collage of six photographs showing what happened during this defrost cycle. The six pictures in this figure cover the events of the first 40 seconds of the defrost cycle. “A” shows layers of frost on the surface of the heat exchanger; “B” through “D” show the layers of frost being detached from the surface of the heat exchanger and moving away; “E” shows the time when the layer from the right side fell off; “F” shows the time when the layer from the left also fell off, and it was also the end of the defrost cycle.

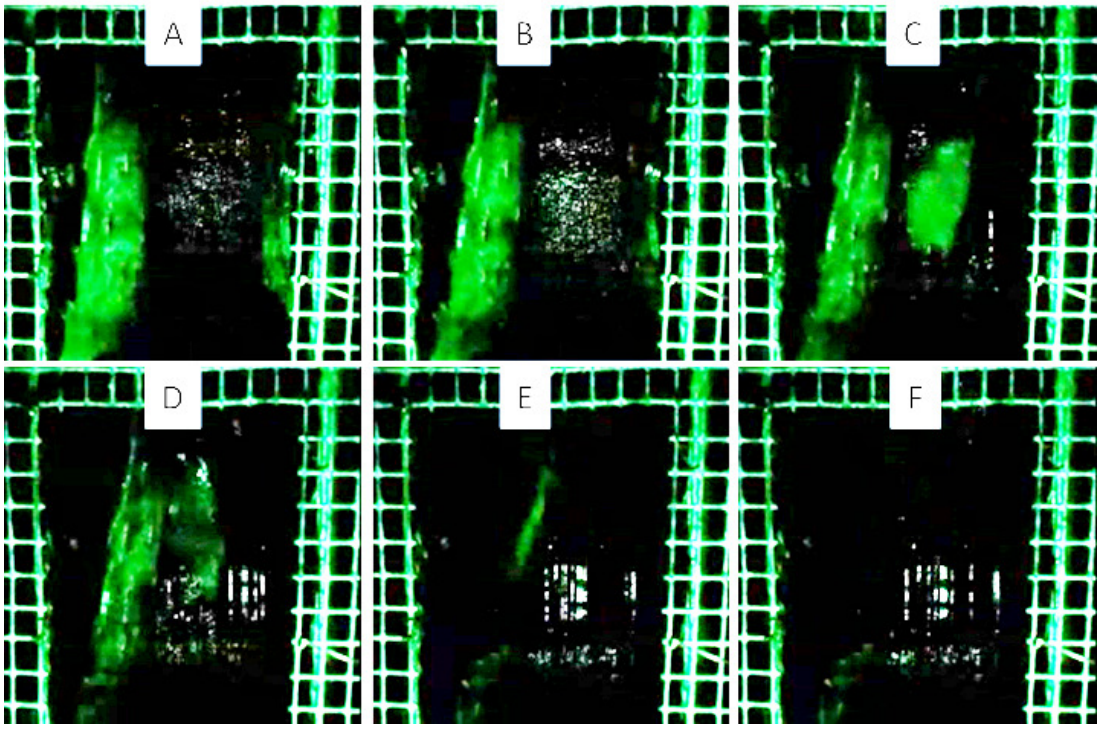

Figure 25: Visual evidence to show that layers of frost can be dislodged from the coil surface without providing the thermal energy to melt it. (A) The frost layers at the start of the defrost cycle (B) The layers getting detached (C) The layer from the right corner gets detached and moves towards the center (D) Both layers about to fall off without melting (E) The right layer has fallen off (F) The left layer also falls off

The working fluid in the defrost cycle initiates the melting of frost, but before all the frost could be melted, the reverse air dislodges some portions of the frost. Even though this experiment was set up to run defrost cycles for 1 minute intervals, it was observed that 40 seconds was sufficient to complete the defrost with the continuous use of the reverse air fan during the defrost cycle.

6.2. Modified time based defrost strategy

Figure 26 shows the variation of pressure drop across the heat exchanger with time for the experiments that were set up based on the modified time-based defrost cycle

discussed in section 5.3. In this experiment the set point for the differential pressure to initiate the defrost cycle was 30 Pa.

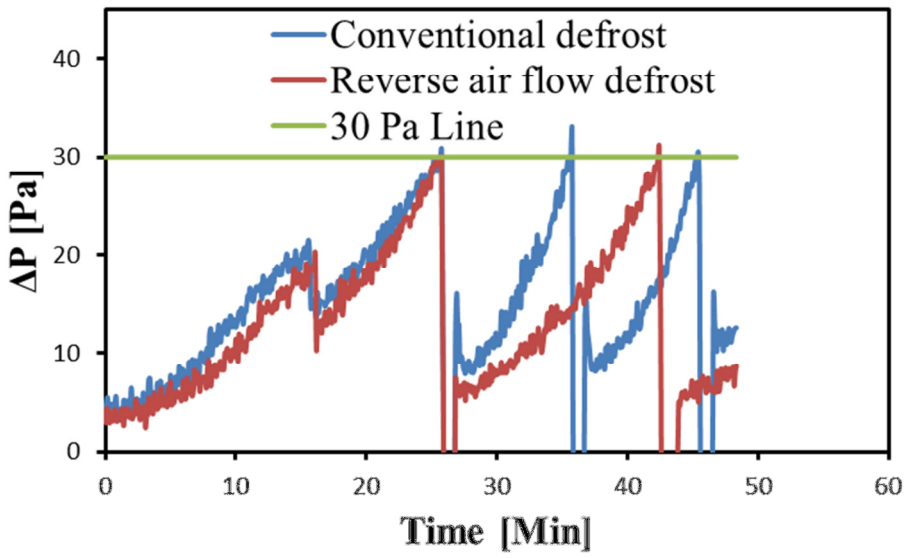

Figure 26: Pressure drop variation in the time based defrost strategy during the frost formation and defrost cycles for conventional and reverse air flow methods with defrost cycle initiated at ΔP = 30 Pa

From the comparison of the conventional method with the reverse air fan method, it can be observed that the frost growth profile in the first cycle was the same for both experiments. The conventional method needed more defrost cycles in a given time interval of operation as compared to the reverse air flow defrost. The conventional defrost method of operation needed three defrost cycles in 50 minutes, while the reverse air flow defrost method needed two defrost cycles. There are multiple reasons for these differences in the number of defrost cycles needed in the same duration of operation. The first reason is that with the use of reverse air fan during the defrost cycle some part of the frost can be dislodged without melting it, as demonstrated in section 6.1. The second

reason is that in the conventional defrost method the residual water droplets after the 40 seconds defrost process depend on gravity forces to fall off the coil surface; this evidently is a slow process. In contrast, in the case of the reverse air fan method the residual water droplets are removed from the coil surface more effectively by the moving stream of air. It was observed that at the end of each 40 seconds defrost cycle, the starting differential pressure for the conventional method was constantly increasing. It seems that the reason for this increasing trend can be associated with the presence of residual moisture on the surface of the heat exchanger. This increase in the starting differential pressure is the third reason for the need for more defrost cycles in the conventional method.

The reason for the residual moisture is twofold. The first reason is 40 seconds is probably insufficient for complete melting of all the frost, and the second reason is that gravitational force on the water droplets is inadequate to overcome the adhesion force for them to fall off on their own.

When the total number of operating hours of a heat pump increases, the difference in the number of defrost cycles between the two methods also increases. This indicates that there is an energy saving opportunity when the reverse air flow fan is used in the defrost cycle.

Since the experiment was set up in such a way that the heat transfer from the working fluid was in a single-phase mode, the thermal energy supplied by the working fluid during a defrost cycle can be estimated using Eq.(2) .

$$Q_{defrost} = \sum C_{p\,F} \,.\, \dot{m}_F \,.\, \Delta T . \Delta t \qquad (2)$$

where ΔT is the differential temperature measured using the differential thermocouple and Δt is the time interval between subsequent data collected by the data logger (5 seconds). The summation in Eq.(2) adds the defrost heat energy for the entire duration of a defrost cycle.

In the case of the reverse air fan defrost method, the electrical energy due to the fan operation during a defrost cycle can be calculated using the fan current and DC voltage data as shown in Eq. (3) .

$$E = \sum V_{DC} \, . \, I \, . \Delta t \tag{3}$$

The total defrost energy during a defrost cycle is calculated as the sum of the thermal energy and the electrical energy as given by Eq.(4) .

$$\text{Total defrost energy} = Q_{defrost} + E \tag{4}$$

Table 6 shows the energy utilized during the defrost cycle for the two methods.

Table 6: Energy utilization in the modified time based defrost strategy for the conventional and reverse air fan defrost methods at the differential pressure set point of 30 Pa

Experiment Name	Differential Pressure (Pa)	Reverse Air Fan Velocity (m/s)	Fan Electrical Energy (kJ)	Defrost Thermal Energy (kJ)	Total Defrost Energy (kJ)
Reverse Air fan Defrost	30	5.5	4.20	5.23	9.43 ±0.17
Conventional Defrost	30	0.0	0	7.89	7.89 ±0.43

The total defrost energy per defrost cycle of the reverse air flow defrost is higher than the conventional defrost. The energy requirement for a given time period of operation of the heat pump can be estimated using Eq. (5) .

$$\text{Energy requirement} = \text{Total defrost energy} \times \text{Number of defrost cycles in the period of operation} \quad (5)$$

For the two experiments shown in Figure 26, the energy requirement can be estimated using the information in Table 6. Thus the energy requirement for the conventional defrost method would be 24 kJ for three defrost cycles in 50 minutes of operations, and for the reverse air fan defrost method the energy requirement would be 19 kJ for two defrost cycles for the same duration of 50 minutes. This establishes an energy saving opportunity when the defrost cycles are run with the use of the reverse air fan method. The energy savings is due to the reduction in the number of defrost cycles needed in a given period of operation.

6.3. Control based defrost strategy – Above freezing environment

Figure 27 shows the differential temperature versus time, and Figure 28 shows the differential pressure versus time for the conventional defrost method for the above-freezing environment with the control-based defrost strategy.

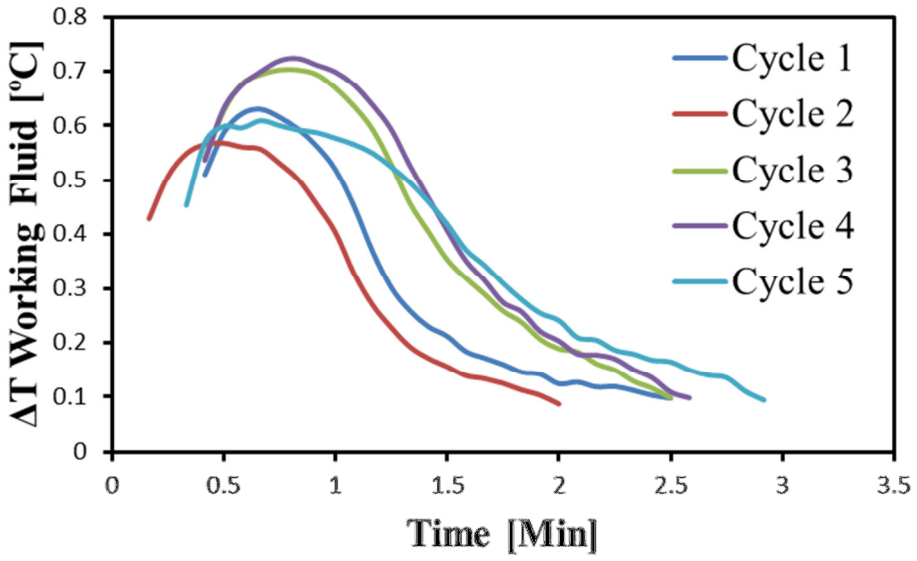

Figure 27: Differential temperature variation for conventional method in above freezing environment using control based defrost strategy with the defrost cycle termination criteria set to $\Delta T < 0.1^{\circ}C$

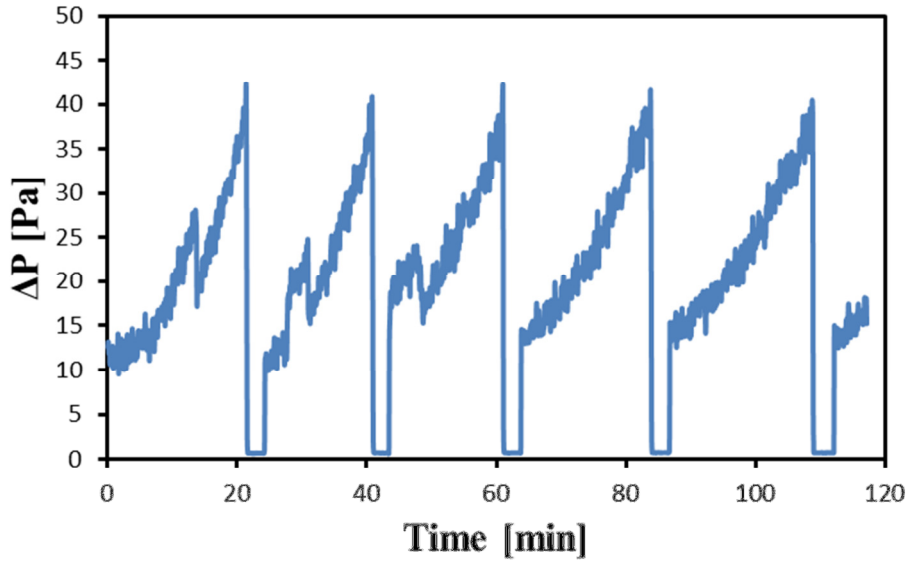

Figure 28: Differential Pressure variation for conventional method in above freezing environment using the control based defrost strategy with the defrost cycle termination criteria set to $\Delta T < 0.1^{\circ}C$

Using Eq (2) it was estimated that the thermal energy supplied during the defrost cycle was 12.6 ± 0.46 kJ per defrost cycle. As seen in Figure 27, , it took about 2.5 to 3 minutes

to reach the $\Delta T < 0.1$ ºC criterion. This supports the observation in section that 40-second time interval for defrost experiments of the time-based strategy is insufficient for completing defrost and getting rid of the entire frost and/or water droplet.

Additional experiments were run such that the defrost termination criteria was changed from $\Delta T < 0.1$ ºC to higher numbers such as $\Delta T < 0.2$ ºC and $\Delta T < 0.3$ ºC. This can be considered as a way to reduce the thermal energy supplied to melt the frost. The idea was to reduce the thermal energy supplied during the defrost cycle of the conventional defrost method so as to determine whether the thermal energy was melting the frost or adding heat to the water droplets after melting.

Figure 29 & Figure 30 show the differential pressure across the heat exchanger versus time plot for these two experiments; a close look at these two plots indicates that the value of ΔP at the end of each defrost cycle was the same as the experiment with $\Delta T <$ 0.1 ºC criteria.

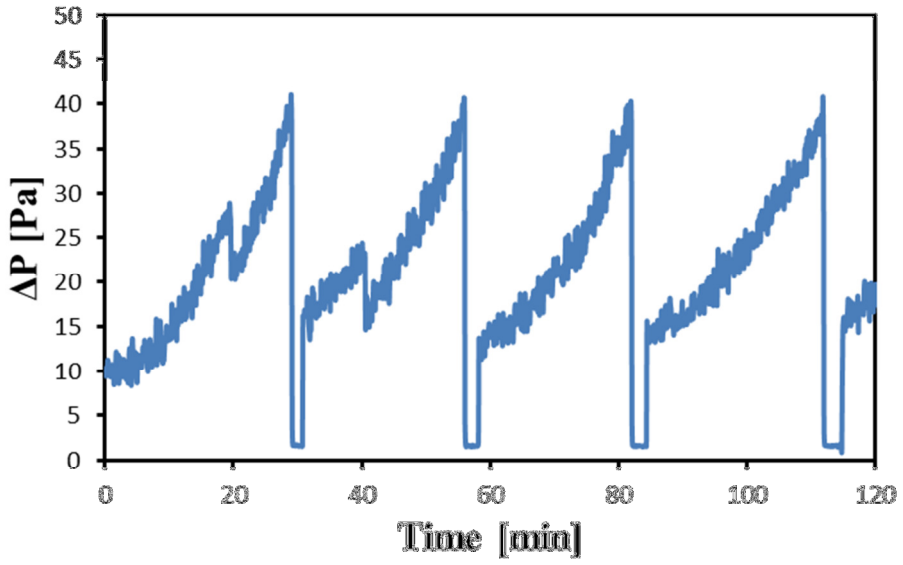

Figure 29: Differential pressure variation for conventional method in above freezing environment using the control based defrost strategy with the defrost cycle termination criteria set to $\Delta T < 0.2^{o}C$

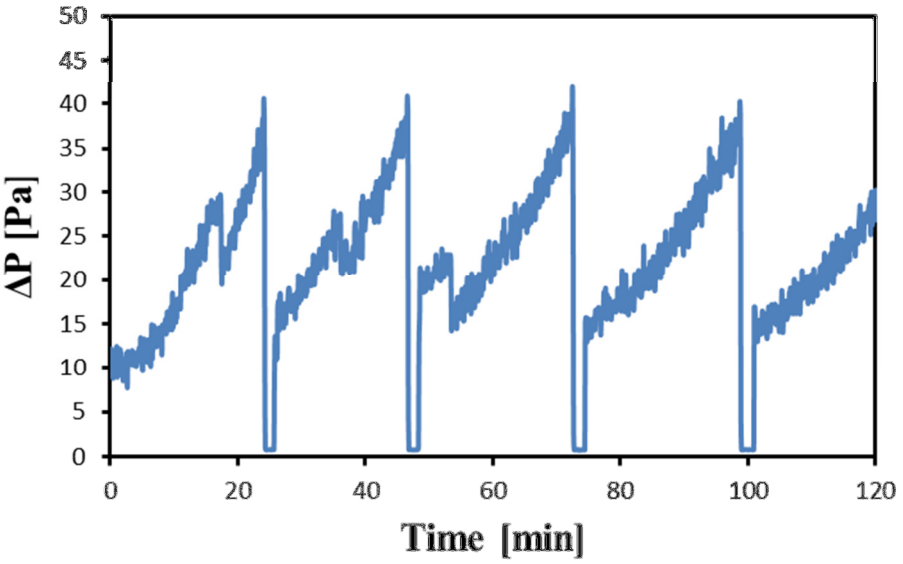

Figure 30: Differential pressure variation for conventional method in above freezing environment using the control based defrost strategy with the defrost cycle termination criteria set to $\Delta T < 0.3^{o}C$

This indicates that the last part of the thermal energy supplied did not melt the frost but instead just added heat to the water droplets that did not fall off with gravitational force. This further suggests that the thermal energy supplied during the defrost cycle of the conventional method can be reduced without any impact on the differential pressure versus time plot. The differential pressure versus time characteristic will be better when the draining is improved. It will be worse when the frost does not melt completely.

The differential temperature versus time plots of the above experiments, i.e., Figure 27 can be viewed as having two distinct regions: the top region with a dome-like shape and the bottom region with a steep dropping trend. The top region seems to be the region where the latent energy was supplied to melt the frost; the latter steeper region seems to be the region where the temperature of the water droplets started to increase to match the temperature of the working fluid. The differential temperature versus time plot shows that the differential temperature rises at the start of the defrost cycle. This is because of the transition from the simulated heating cycle to the simulated defrost cycle. When the valve is switched to change from the cold bath to warm bath, a transition occurs. This causes the appearance of the initial rising trend for all defrost cycles.

The next idea was to see if supplying a blast of air could clean the coil surface better. This led to the formation of the reverse air flow defrost method for the control-based defrost strategy. The idea was to use a ΔT set point which would be as high as practically possible in the experiment for the defrost cycle termination criteria and then use reverse air fan for 20 seconds at the end of the defrost cycle. The reverse air fan used in the experiment took approximately 20 seconds to overcome all resistance and inertia and

reach its full current value of 1.85 A under clean conditions. This was the reason for selecting 20 seconds.

The first reverse air fan defrost experiment used $\Delta T < 0.5$ ℃ as the termination criteria, and a blast of reverse air was supplied to clean away the coil surface for the last 20 seconds of the defrost cycle (i.e. after achieving the ΔT criteria). From the data of this experiment, it was found that the total defrost energy per defrost cycle, as defined in Eq.(4) for this experiment, was 11.3 kJ. Additional experiments indicated that the best result in terms of least total defrost energy was obtained with $\Delta T < 0.54$ ℃ as the criteria followed by 20 seconds of reverse air.

Figure 31 and Figure 32 show the corresponding differential temperature versus time and differential pressure versus time plots. The total defrost energy per defrost cycle as defined in Eq.(4) reduced to 9.5 ± 0.47 kJ.

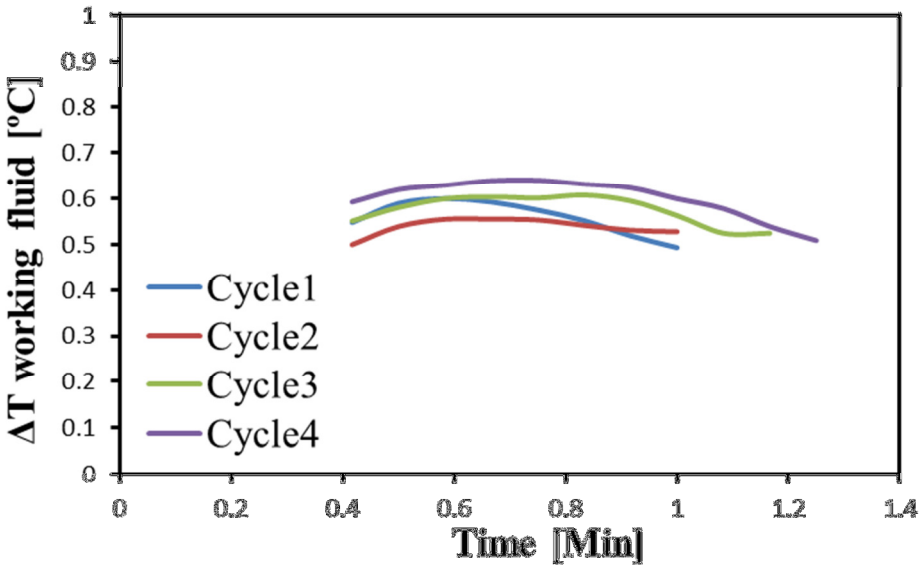

Figure 31: Differential temperature variation for reverse air method in above freezing environment using the control based defrost strategy at the termination criteria of ΔT < 0.54ºC

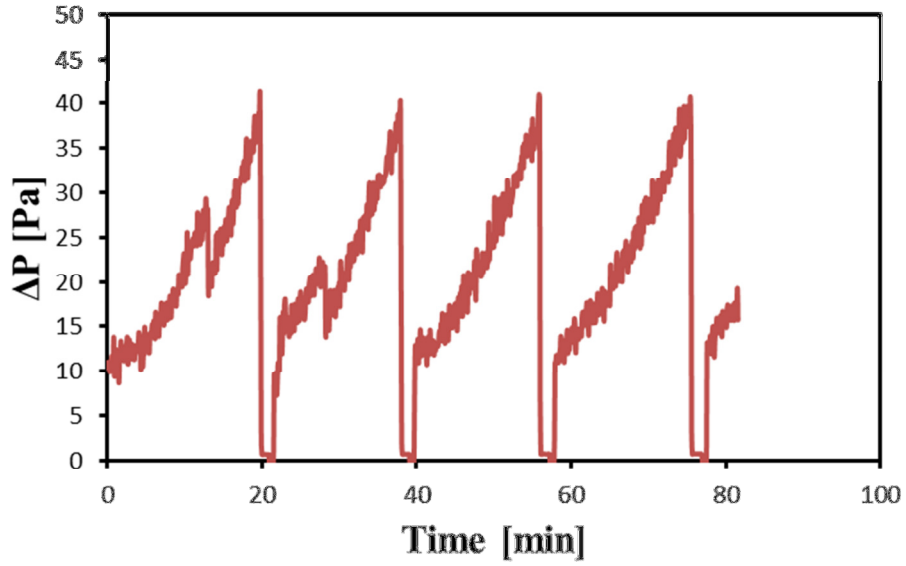

Figure 32: Differential Pressure variation for reverse air method in above freezing environment using the control based defrost strategy at the termination criteria of ΔT < 0.54ºC

An energy savings of 24 ± 4 % was seen when the conventional defrost experiment with

ΔT < 0.1° C criteria was compared with the ΔT < 0.54 ºC criteria followed by 20 seconds

of reverse air defrost case. In general, increasing the ΔT set point to numbers larger than 0.1 ºC and using a blast of reverse air provided an energy savings.

6.4. Control based defrost strategy – Below freezing environment

When the temperature of the outdoor air drops far below 0 ºC, the problem of frost reduces because the moisture content in air drops at such low temperatures. A lower bound of -5 ºC has been identified for the worst freezing conditions[1]. The experiments of this section show the energy saving opportunities when the environment was maintained below 0 ºC.

Table 5 shows the experimental test conditions, and section 5.4 describes the control-based defrost strategy.

Figure 33 and Figure 34 show the differential temperature versus time and differential pressure versus time plots for the conventional method. It was seen that the value of differential pressure at the end of each subsequent defrost cycle kept on increasing. There was a rising trend on the differential pressure versus time plot in spite of the defrost cycle being terminated at $\Delta T < 0.1$ ºC.

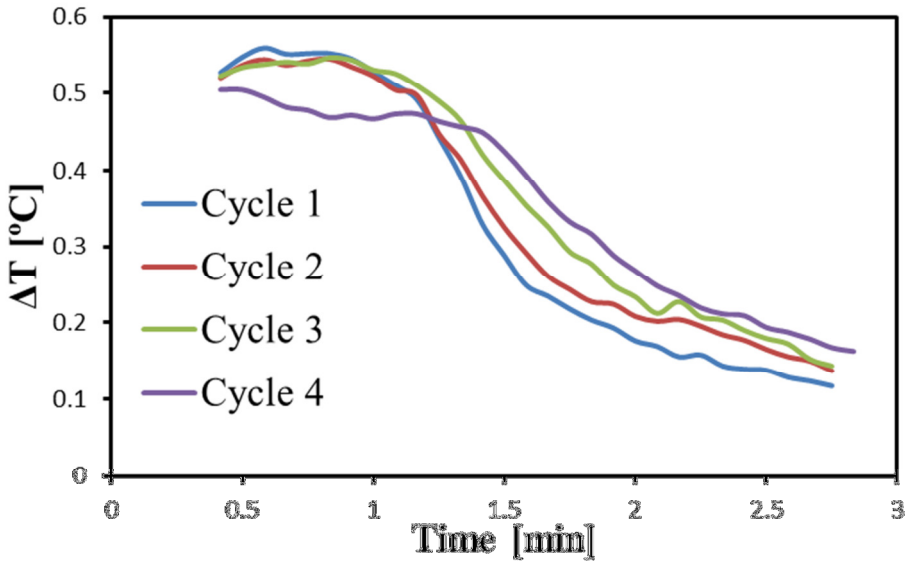

Figure 33: Differential temperature variation for conventional method in below freezing environment using the control based defrost strategy with the defrost cycle termination set point at $\Delta T < 0.1^{\circ}C$

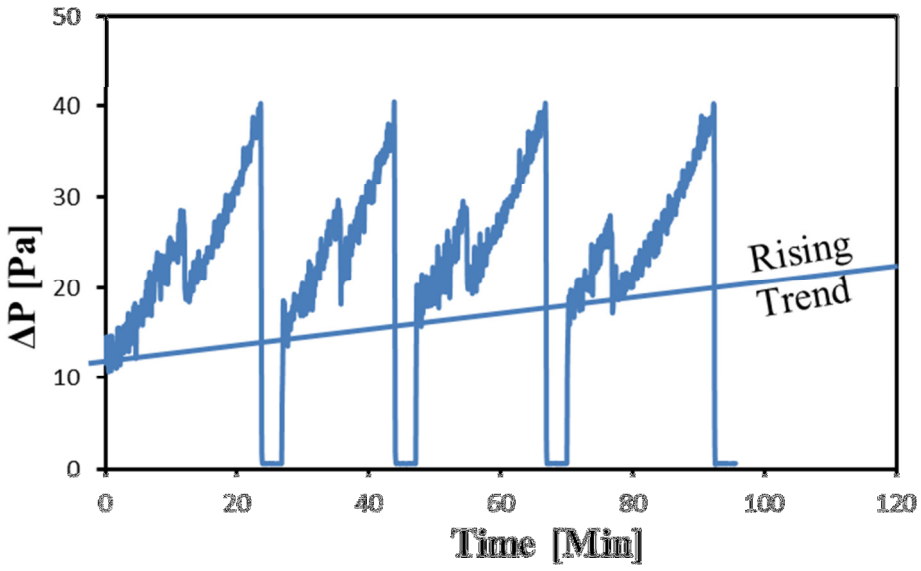

Figure 34: Differential pressure variation for conventional method in below freezing environment using the control based defrost strategy with the defrost cycle termination set point at $\Delta T < 0.1^{\circ}C$

The reason for this trend is that during defrost cycle of the conventional method, the water droplets do not fall off easily. These residual water droplets refreeze rapidly in the next simulated heating cycle. The refreezing starts the moment the cycle changes from simulated defrost to simulated heating mode. For these below-freezing experiments, the refreezing was not only due to the sub-freezing temperature of the fin surfaces, which in turn is due to the cold working fluid in the simulated heating cycle, but also due to the environment, which was below freezing temperatures. In the case of the above-freezing experiment, refreezing occurs due to the sub-freezing fin surface temperature, while the environment does not contribute to the refreezing. Thus the refreezing is not instantaneous.

The total defrost energy was calculated using Eq. (4) , as 17.08 ± 0.65 kJ per defrost cycle. The frost had to melt in the defrost cycle using the heat rejected from the working fluid, but there was no control on the water droplets after the melting process. It became clear that when the valves were switched to return to the simulated heating cycle, the water droplets froze again. In order to improve this situation, an improved sequence of operation was proposed such that the thermal mass of the heat exchanger metal could be used effectively.

Table 7: Proposed sequence of operation for the below freezing experiment with conventional method of defrost using the control based defrost strategy to make use of the metal thermal mass

Step	Current Industrial Sequence	Proposed Sequence
1	Reach ΔP of 40 Pa	Reach ΔP of 40 Pa
2	Turn (forward)fan off	Turn (forward)fan off
3	Switch valve to reverse cycle, (start of defrost cycle)	Switch valve to reverse cycle, (start of defrost cycle)
4	Reach ΔT of 0.1° C	Reach ΔT of 0.1° C

5	Switch valve, simulated heating cycle	turn (forward) fan on
6	turn (forward) fan on	Switch valve, simulated heating cycle

Table 7 shows a comparison of the current industrial sequence of operation and the proposed sequence of operation. In this table the change between the current industrial practice and the proposed sequence is in the last two steps where the order of events after the criteria to terminate the simulated defrost cycle is met. The general idea was that the environment temperature was higher than the working fluid temperature for evaporation to occur during the heating cycle. Thus, when terminating the defrost cycle and switching back to the heating cycle, if the fan is turned on first and the value switched next, then the residual water droplets that are on the surface of the heat exchanger get extra time at a relatively higher temperature before they refreeze. Additionally this creates an opportunity for the moving stream of ambient air to interact with the residual water droplets when the working fluid inside the heat exchanger is still from the warm bath. In the current industrial sequence, when the criteria to terminate the defrost cycle is reached the valve is switched to invert the cycle and go into the heating cycle first, and the fan is turned on at the end. In doing so, the heat exchanger is cooled by the cold working fluid of the simulated heating cycle, which is lower in temperature than the ambient air. Refreezing of the residual water droplets happens more quickly in this case. Thus, when the fan is turned on the moving stream of air does not get an opportunity to interact with warmer water droplets and create an opportunity to dislodge them.

The proposed sequence of operation was used in an experiment. Figure 35 and Figure 36 show the differential pressure versus time and differential temperature versus time plots, respectively.

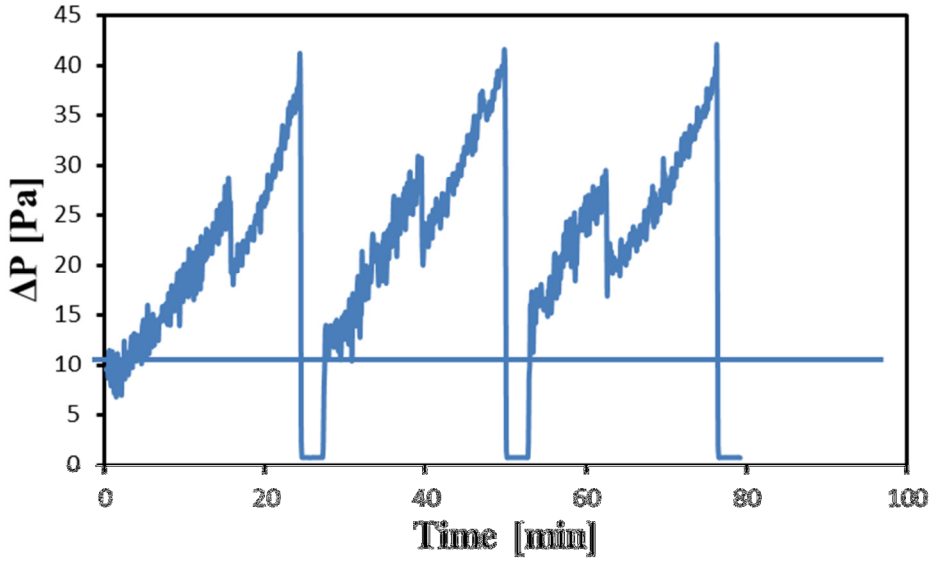

Figure 35: Differential pressure variation - proposed sequence; conventional method; below freezing environment using the control based defrost strategy and keeping the defrost termination criteria as $\Delta T < 0.1^{\circ}C$

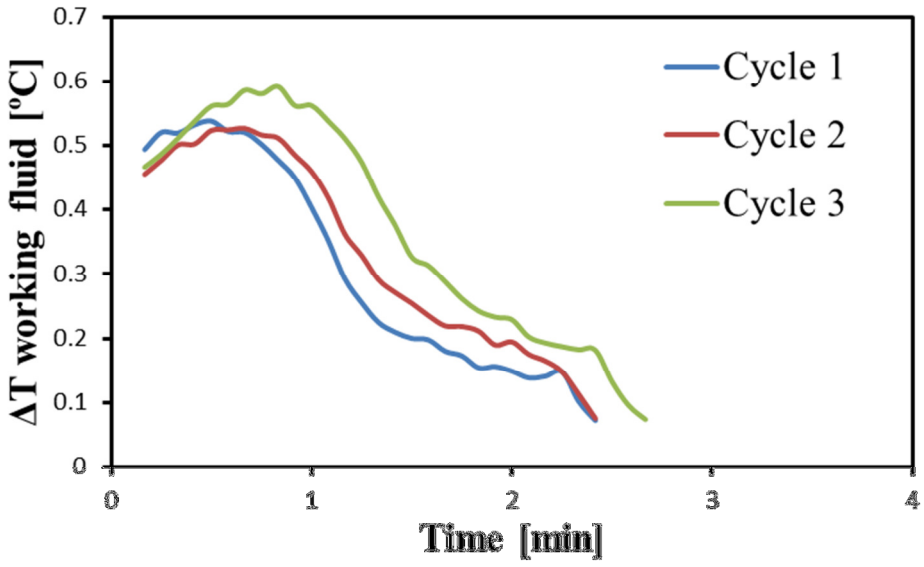

Figure 36: Differential temperature variation - proposed sequence; conventional method; below freezing environment using the control based defrost strategy and keeping the defrost termination criteria as ΔT <0.1ºC

The differential pressure across the heat exchanger after the defrost cycles was consistent and there was no rising trend. The key seems to be in the fact that air flow started when the working fluid inside the coil was still from the warm bath, permitting the use of thermal mass. The total defrost energy calculated using Eq. (4) was 19.4 ± 0.72 kJ per defrost cycle.

Since making use of the thermal mass of the outdoor coil by changing the sequence of operation improved the defrost process, further improvements using reverse air fan were also explored. The reverse air fan method used in the above-freezing environment experiments was adopted in the below-freezing environment. The ΔT set point value was increased to 0.3 ºC, and a blast of reverse air was used for 20 seconds, but it was seen that

the defrost cycle could not be completed with this method. Figure 37 shows the differential pressure versus time plot for this experiment.

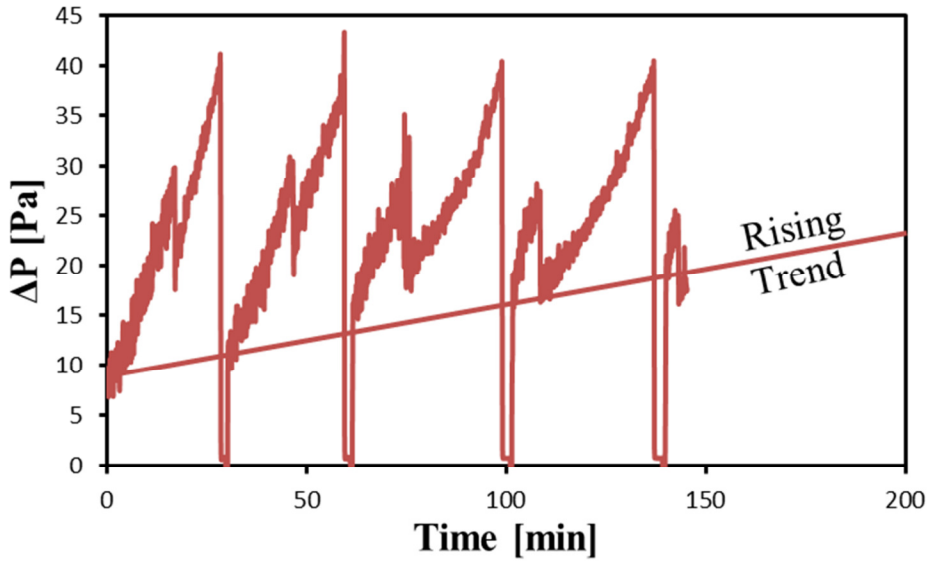

Figure 37: Differential pressure variation in a reverse air fan method; below freezing environment; using control based strategy with the defrost termination criteria as ΔT <0.3ºC

The differential pressure values at the end of subsequent defrost cycles showed a rising trend. It was concluded that for the below-freezing environment any reduction in the amount of thermal energy supplied during the defrost cycle resulted in incomplete defrost cycles.

A new sequence of operation was proposed for the reverse air fan method such that the thermal mass of the outdoor coil could be used. Table 8 shows this proposed sequence.

Table 8: Proposed sequence of operation for the reverse air fan method in the below freezing environment using the control based defrost strategy

Step	Proposed Sequence for below freezing case
1	Reach ΔP of 40 Pa
2	Turn (forward)fan off

3	Switch valve to reverse cycle, (start of defrost cycle)
4	Reach ΔT of 0.1 C
5	Turn on reverse air 20 sec
6	Switch valve to neutral
7	Turn reverse off
8	Turn forward fan on
9	Switch valve for simulated heating cycle

As compared to the above-freezing environment, the defrost cycle termination criteria was not modified in the below-freezing environment. Following the idea of the sequence proposed to improve the conventional defrost method, this sequence allowed the reverse air to flow over the heat exchanger at a time when there was warm fluid circulating inside the coil.

Figure 38 and Figure 39 show the differential pressure versus time and differential temperature versus time plots for this proposed improvement.

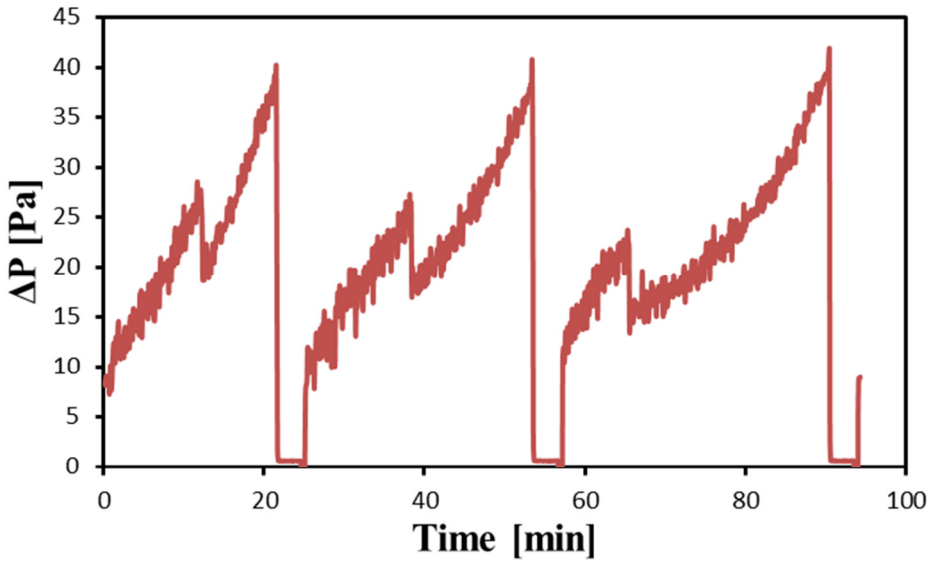

Figure 38: Differential pressure variation - proposed sequence; reverse air method; below freezing environment using the control based defrost strategy and keeping the defrost termination criteria as ΔT <0.1ºC

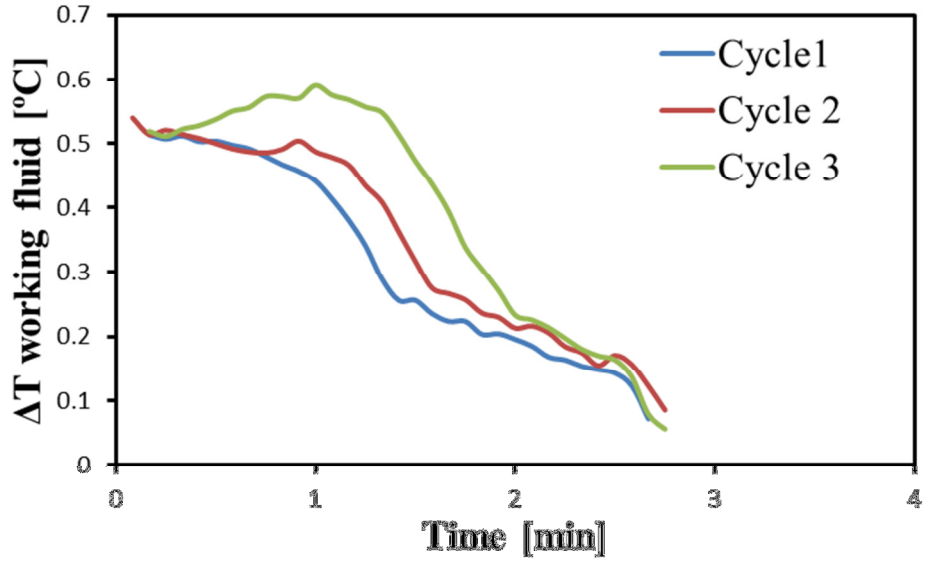

Figure 39: Differential temperature variation - proposed sequence; reverse air method; below freezing environment using the control based defrost strategy and keeping the defrost termination criteria as ΔT <0.1ºC

Use of this sequence of operation with the reverse air fan method ensured that there was no rising trend in the differential pressure versus time plot. The total defrost energy calculated using Eq.(4) was estimated as 21.0 ± 0.8 kJ per defrost cycle. Clearly the total defrost energy had increased because the use of the reverse air fan added the electrical energy component. The thermal energy used in the defrost cycle remained the same because the ΔT set point was still at 0.1 ºC, which was similar to the conventional defrost method. The benefit of using the reverse air fan at a higher total defrost energy per cycle is that the number of defrost cycles needed in a given time period was reduced.

It can be seen from Figure 38 that it takes about 95 minutes for three cycles, whereas it takes about 80 minutes for three cycles in Figure 35. Using this information and Eq. (5) , the energy requirement was found for these two experiments, and the energy saving was estimated as 8% when reverse air defrost with the new sequence of operation was used instead of the conventional method.

6.5. Control based defrost strategy – Using the forward fan during defrost cycle

An experiment was set up to evaluate the effect of using the air flow in the normal direction instead of the reverse direction. This experiment was set up in the above-freezing environment using the control-based defrost strategy. The test conditions are summarized in Table 4. The defrost cycle was initiated when the differential pressure across the heat exchanger reached 40 Pa. Defrost cycle termination criteria was selected as $\Delta T < 0.54$ ºC, which is the same as the result discussed in section 6.3 for the reverse air method. When this termination criterion was reached, the fan was used in the forward

direction for the same 20 seconds. Figure 40 shows the differential pressure versus time plot for this experiment.

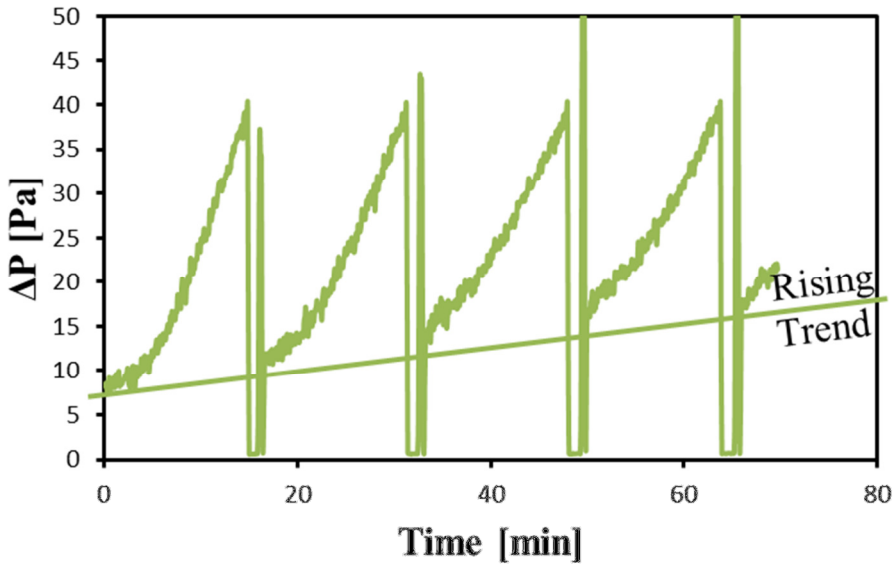

Figure 40: Differential pressure variation in the above freezing environment using forward fan in a control based defrost strategy experiment

It was seen that the differential pressure values at the end of the defrost cycles showed a rising trend indicating that defrost was not complete in this case. Because of the direction of the air flow, it appears that the forward fan pushed the frost into the fin area of the coil, causing this rising trend. In the case of the reverse air fan, the air pushed the frost away and out of the coil. This result indicated that use of the forward fan during the defrost cycle was not a good choice.

6.6. Control based defrost strategy – ASHRAE recommended defrost cycle termination set point

ASHRAE recommends that the defrost cycle should be terminated when the temperature of the refrigerant flowing out of the heat exchanger after defrosting rises to 20 ºC (68 ºF) [1].

Table 4 and Table 5 lists the test conditions for the experiments described in section 6.3 and 6.4. The warm bath temperature in these experiments was 8 ºC, selected based on the temperature lift criteria discussed in section 5.4. However, under actual operation condition of heat pumps the temperature of the refrigerant increases during the course of the defrost cycle and the typical end temperature would be 20 ºC (68 ºF). [1]

The energy needed in the defrost cycle to raise the refrigerant temperature from the initial value to the final value of 20 ºC (68 ºF) has not been accounted for in the experiments of sections 6.3 and 6.4. The defrost termination criteria of $\Delta T < 0.1$ ºC used in the experiments of sections 6.3 and 6.4 capture only the thermal energy supplied to melt the frost. The refrigerant temperature rises after this point.

It is desired to have an estimate of the thermal energy needed to melt the frost and then to raise the refrigerant temperature to 20 ºC (68 ºF). This estimate would be the real thermal energy used if the ASHRAE recommended defrost cycle termination criteria is used.

Based on the interpretation of the control strategy made in section 5.4, if the warm bath temperature is selected as 20 ºC (68 ºF), then, at the defrost cycle termination condition of $\Delta T = 0.1$ ºC, it would be safe to say that the end condition as recommended by ASHRAE is matched. Thus, selecting a warm bath temperature of 20ºC would effectively give us an estimate of thermal energy which would include both the frost melting part and the refrigerant temperature increasing part.

Two experiments, one for above-freezing conditions and another for below-freezing conditions were run with warm bath temperature at 20 ºC. All other experimental conditions were unchanged in Table 4 and Table 5. The total defrost energy per defrost cycle calculated using Eq. (4) from these experiments is summarized in Table 9.

Table 9: Total defrost energy calculated using the ASHRAE recommended defrost cycle termination criteria for the above and below freezing environments using the control based defrost strategy.

Above Freezing Experiment	Below Freezing Experiment
21.65 ± 0.84 kJ	30.35 ± 1.11 kJ

The total energy increases as compared to the experiments of sections 6.3 & 6.4. Table 10 shows a comparison of the results and the energy savings calculated form these experiments. The comparison in Table 10 indicates that the current ASHRAE recommendation is very conservative and there is an opportunity to save energy.

Table 10: Total defrost energy for the control based defrost strategy experiments and the energy savings calculated as a comparison of the ASHRAE recommended set point experiment against the proposed reverse air fan method for both above and below freezing environments

Environment	Control Based Defrost Experiment Name	Total Defrost Energy per defrost cycle (kJ)	Energy Savings (%)
Above Freezing Environment	ASHRAE Set Point	21.65 ± 0.84	56
	Conventional Method	12.6 ± 0.46	
	Reverse Air Method	9.5 ± 0.47	
Below Freezing Environment	ASHRAE Set Point	30.35 ± 1.11	31
	Conventional method	19.4 ± 0.72	
	Reverse Air Method	21.0 ± 0.8	

6.7. Continuous use of reverse air fan in control based defrost strategy

An experiment was conducted with the control strategy described in section 5.5. Figure 41 & Figure 42 show the differential pressure versus time and differential temperature versus time plot for this experiment.

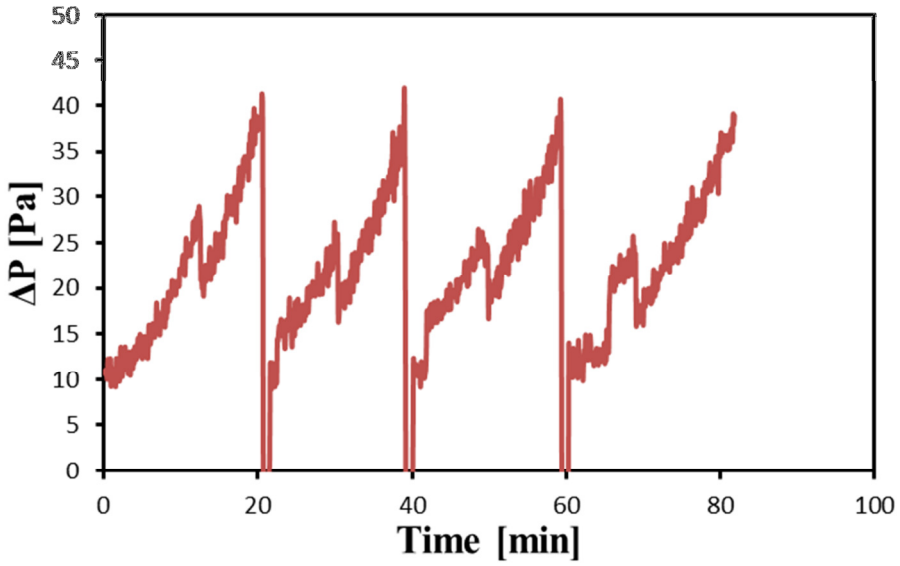

Figure 41: Differential pressure variation with continuous use of reverse air fan during defrost in above freezing environment for the control based defrost strategy where fan current is the process parameter for termination of defrost cycle.

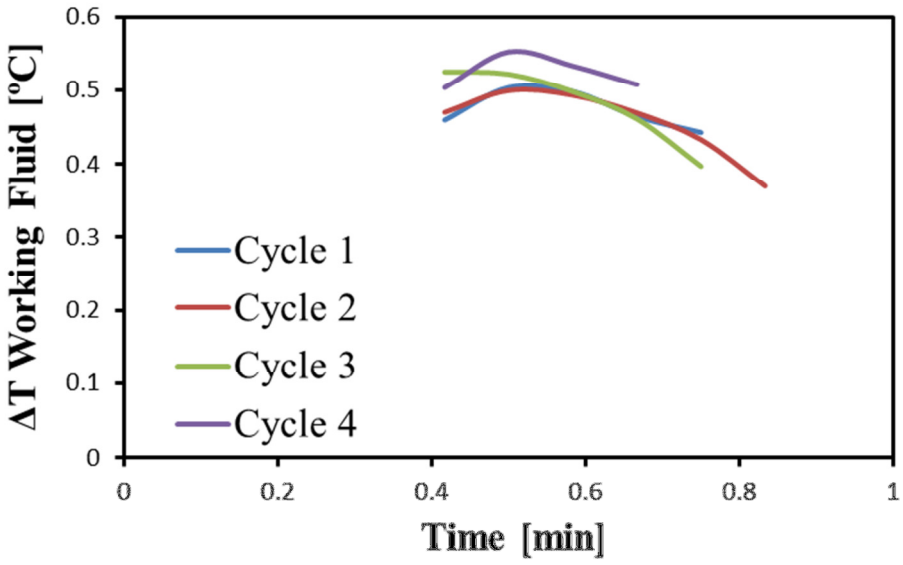

Figure 42: Differential temperature variation with continuous use of reverse air fan during defrost in above freezing environment for the control based defrost strategy where fan current is the process parameter for termination of defrost cycle.

From the data of this experiment the total defrost energy per defrost cycle was estimated using Eq. (4) as 8.4 ± 0.36 KJ. An Energy savings of 33 ± 4 % per defrost cycle was estimated when this was compared to the conventional method experiment run with the control based strategy.

An energy savings of 61 % was estimated when the result of this experiment was compared with the result of experiment run with ASHRAE recommend termination set point criteria.

From this result it is evident that use of reverse air fan continuously during the defrost cycle creates the maximum energy saving opportunity in the above freezing environment.

6.8. Varying air velocity during frost formation

Three experiments were conducted with the velocity of the forward fan set to 0.8 m/s, 2 m/s and 3 m/s. Figure 43 shows the differential temperature versus time plots.

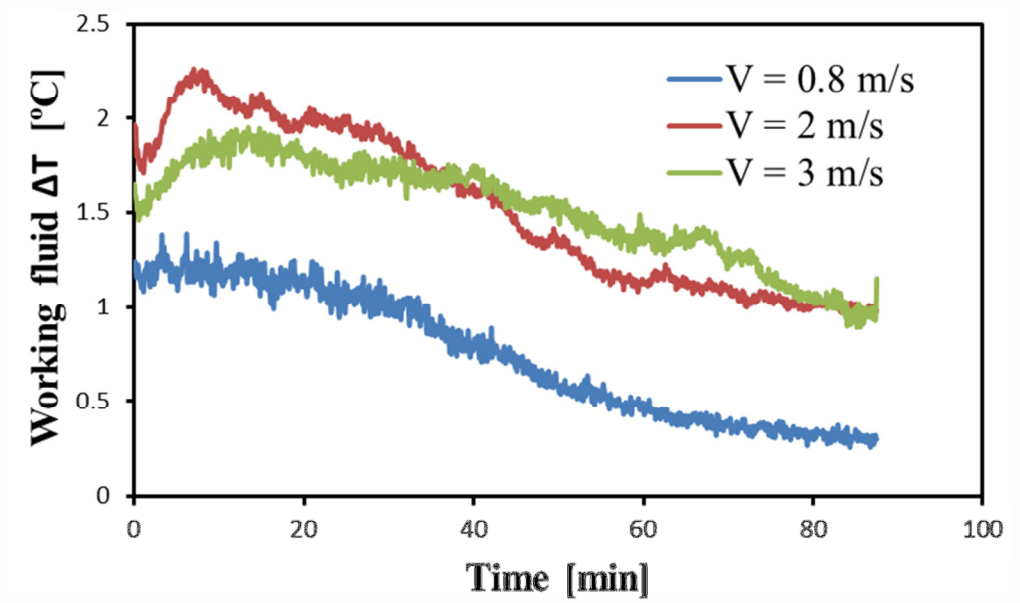

Figure 43: Differential temperature variation at different forward fan velocities in the above freezing environment for a 90 minute frost formation experiment

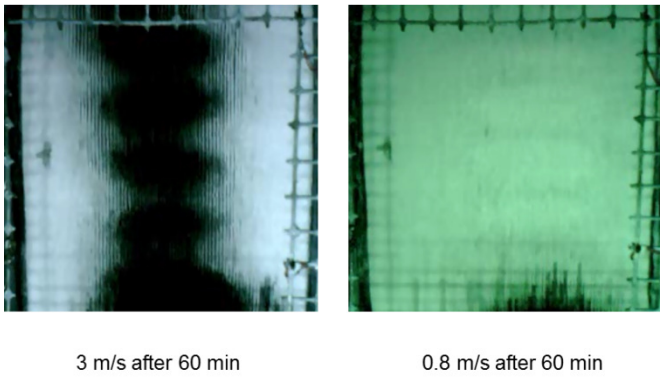

Figure 44: Visual evidence for slower frost growth with increase in air velocity during the frost formation period.

It is seen that at velocities of 2 m/s and 3 m/s the differential temperature is higher than at velocity of 0.8 m/s. This higher differential temperature indicates that the heat transfer rate is higher because heat transfer is given by Eq. (2). This suggests that the frost growth is slower at higher velocities of air flow during the frost formation period. Figure 44 provides visual evidence to support the fact that frost growth rate is retarded at higher velocity of air flow.

It is seen that the differential temperature curve of the 2m/s experiment crosses path with the curve of the 3 m/s experiment at two points. This suggests that the effectiveness of this method does not improve beyond a certain increase in the air velocity.

7. ERROR PROPAGATION

The built in Error propagation function of EES was set up to estimate uncertainty of calculated parameter. The function was set up using the uncertainty of measurement and measuring instrument accuracy [19, 20]. Figure 45 & Figure 46 are screen shots from the EES program.

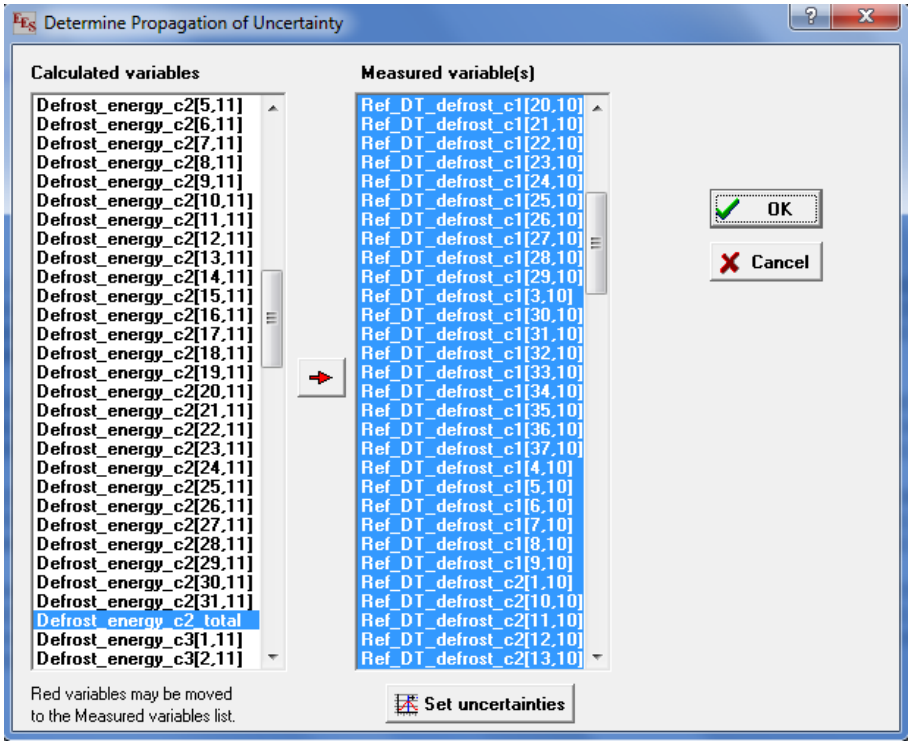

Figure 45: Variable selection window in the EES program for setting up the error propagation to estimate the uncertainty in the calculated parameters.

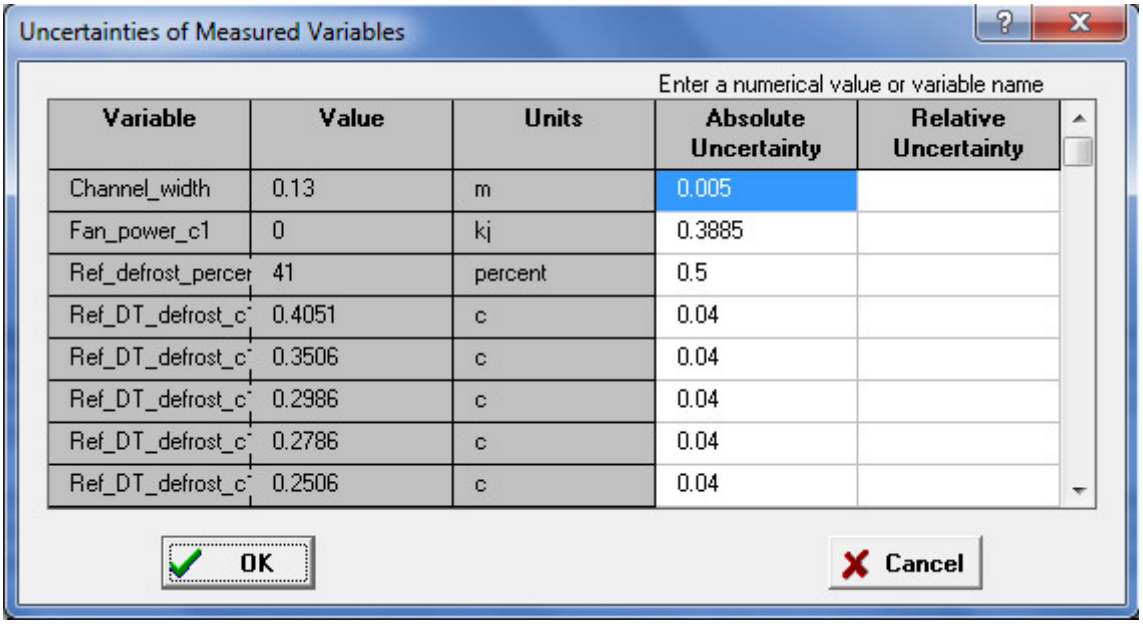

Figure 46: Window where the absolute uncertainty for each of the measured value can be set based on the measuring instrument accuracy and measurement uncertainty

Figure 45, shows the window where the calculated and measured variables are listed. Figure 46 is the window where the absolute uncertainty for each measured value is set. The Measurement instrument catalogs provide the value for the accuracy of measurement. These values are used for the absolute uncertainty in Figure 46. For the scales where the measurements are manually read, such as the float type flow meter, the least count values are used as the absolute uncertainty [19, 20].

8. SUMMARY & CONCLUSIONS

Use of a reverse air fan during the defrost cycle provides energy savings for both above and below freezing environments. Visual evidence and experimental data showed that frost can be dislodged without melting with the use of a reverse air fan.

Two prominent defrost strategies, time-based defrost and control-based defrost were adopted and modified to identify energy saving opportunities in the defrost cycles. Experiments were conducted to simulate the frost growth and defrost cycle. Energy saving opportunities with the use of reverse air fan was explored for both these control strategies.

Experimental evidence showed that the defrost cycle can be completed with the use of a reverse air fan at defrost termination set points lower than 20 ºC (68 ºF), which in turn leads to energy savings. Experimental evidence also showed that the duration of the defrost cycle can be reduced with the use of reverse air fan during defrosting.

Improvements to the existing control strategy are possible by making changes to the set points of the defrost cycle termination criteria. The control strategy can also be improved by making changes to the sequence of operation.

The entire bandwidth of worst frosting conditions was explored in this study. Using the new methods proposed in this study created energy saving opportunities. The details of total defrost energy for various experiments are tabulated in Table 10.

In summary, the energy savings obtained when using the proposed reverse air fan method as compared to the ASHRAE recommended defrost cycle termination set points was 56% in the above-freezing environment and 31% in the below-freezing environment.

REFERENCES

[1] *HVAC Systems and Equipment*. Atlanta, GA: American Society of Heating, Refrigerating and Air-Conditioning Engineers, Inc., 2004.

[2] "Thermostat & Defrost Controls " in *Heat Pumps* ed. USA: http://www.industrialcontrolsonline.com/, 2014.

[3] K. Muthusubramanian, V. S. Dessiatoun, H. A. Shooshtari, and M. M. Ohadi, "Velocity based defrost and frost inhibition of evaporator coils of heat pumps," presented at the ASME 2014 International Mechanical Engineering Congress & Exposition, Montreal, Quebec, Canada, 2014.

[4] S. Jhee, K. S. Lee, and W. S. Kim, "Effect of surface treatments on the frosting/defrosting behavior of a fin-tube heat exchanger " *International Journal of Refrigeration,* 2002.

[5] P. Vocale, G. L. Morini, and M. Spiga, "Influence of outdoor air conditions on the air source heat pumps performance " in *68th Conference of the Italian Thermal Machines Engineering Association*, 2014.

[6] S. W. Wang and Z. Y. Liu, "A new method for preventing HP from frosting," *Renewable Energy,* 2003.

[7] V. Tudor, M. Ohadi, M. A. Salehi, and J. V. Lawler, "Advances in control of frost on evaporator coils with an applied electric field " *International Journal of Heat and Mass Transfer,* 2005.

[8] J. M. Huang, W. C. Hsieh, X. J. Ke, and C. C. Wang, "The effects of frost thickness on the heat transfer of finned tube heat exchanger subject to the combined influence of fan types " *Applied Thermal Engineering,* 2007.

[9] S. Roy, H. Kumar, and R. Anderson, "Efficient defrosting of an inclined flat surface," *International Journal of Heat and Mass Transfer,* 2005.

[10] Y. Yao, Y. Jiang, S. Deng, and Z. Ma, "A study on the performance of the airside heat exchanger under frosting in an air source heat pump water heater/chiller unit " *International Journal of Heat and Mass Transfer,* 2004.

[11] "Tables of Thermoelectric Voltages and Coefficients for Download -T Type," ed. USA: National Institute of Standards and Technology, 1999.

[12] "Practical Temperature MeasurementApplication note 290," ed. USA: Agilent Technologies, 2012.

[13] ASTM, "Manual on the use of thermocouples in temperature measurement," ed. USA: ASTM Manual Series, 1993.

[14] S. C. West, P. Spencer, and S. Callahan, "A high-precision differential-thermocouple temperature measurement system for the 6.5m MMT primary mirror," ed. MMTO Conversion Technical Memo #99-2, 1999.

[15] J. T. McMullan and R. Morgan, *Heat Pumps*. Bristol: A. Hilger,, 1981.

[16] D. Reay and D. MacMichael, *Heat Pumps Design and Applications - (Practical Handbook for plant managers)*. Oxford, New York Pergamon Press, 1979.

[17] S. Sutphin, *Heat Pumps Installation and Troubleshooting*. Lilburn, GA: Fairmont Press, 1994.

[18] K. H. Zimmerman, "Prospects in Heat Pump Technology & Marketing," presented at the International Energy Agency Heat Pump Conference, Orlando, Florida, 1987.

[19] C. Ratcliffe. Measurement Uncertainty and its Propagation [Online].
[20] J. R. Taylor, *An Introduction to Error Analysis*. Sausalito, California: University Science Books, 1997.